ON ITINERARIES OF TENT MAPS

ROBERT BUCKLEY, YIWANG CHEN, GRACE O'BRIEN, AND ZOE ZHOU

Abstract. We study the Thurston Set, a set introduced by the late William Thurston in [Thu14]. For a tent map with growth rate β, the Thurston Set is the closure of the Galois conjugates of every critically periodic β in $(1, 2]$. In this paper, we compute an approximation of the Thurston Set by creating the largest known public collection of itineraries. This large data set allows us to make new observations regarding the distribution of critically periodic β values within $(1, 2]$ under period length 23, improve the experimental maximum and minimum bounds on the moduli of elements of the set, and, by considering the Thurston Set as a parameter space and its associated attractors, provide evidence in support of an analogous Mandelbrot-Julia Correspondence. In the process, we develop a new technique for storing these itineraries that is memory efficient and produce many helpful visualizations. Finally, we have a new and direct proof that a tent map of slope β has a topological entropy $\log \beta$ that employs methods that make connections between the dynamics of tent maps and a modified Fibonacci sequence.

1. Introduction

1.1. **Overview.** Throughout this paper, we will describe how we compiled the largest known public collection of itineraries[1] corresponding to critically periodic β values of tent maps, a total of 269,017,181 unique itineraries, which take up about 12 GB in memory. In addition, we will explain how we used this new data set to investigate the nature of the Thurston Set through a variety of graphs, images, and animations. Specifically, we have found experimental evidence of an analogy to the Mandelbrot-Julia Correspondence given in [LW19], tightened experimental bounds on maximum and minimum values in the Thurston Set, and created detailed plots of Thurston's Master Teapot. By studying the dynamics of tent maps and using a modified Fibonacci sequence, we provide a new proof that the topological entropy of a tent map with slope β is $\log \beta$. As an additional result, we designed and implemented a new itinerary encoding algorithm to more efficiently compute and store admissible itineraries while still ruling out nearly all reducible itineraries.

The Thurston Set fascinated us for both its visual and historical intrigue. In 2012, Cornell University professor and Fields Medalist, William Thurston,

Date: July 26, 2022.

[1] https://doi.org/10.7302/k7ex-v245

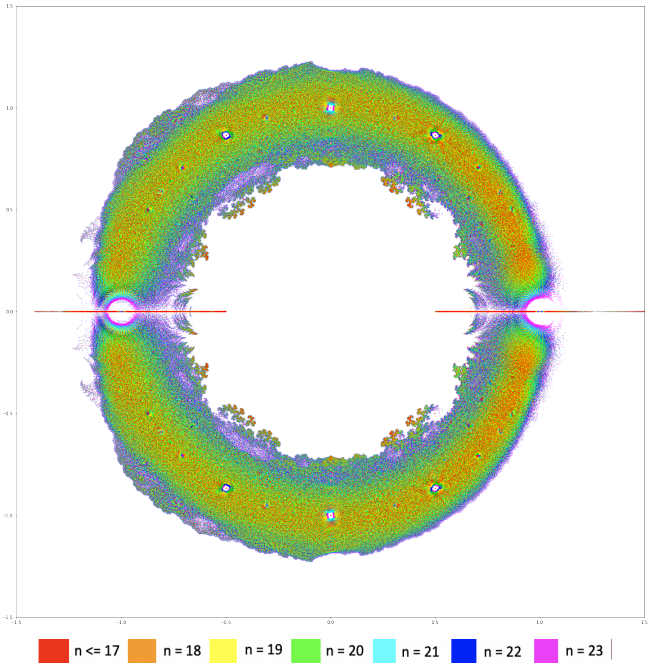

FIGURE 1. An approximation of the Thurston Set, color-coded by orbit length, with points from higher orbit lengths being covered points from lower orbit lengths. See Remark 1.1 for more information.

passed away, but the mathematical mystery that Thurston left behind (Figure 1) has captivated mathematicians ever since ([BDLW19], [CKW17], [Tho16], [Tio20]). Additionally, we are motivated to study the Thurston Set due to its interdisciplinary nature. This set has connections to complex analysis, one-dimensional dynamics, fractal geometry, topology, combinatorics, and number theory, allowing it to be studied from many different perspectives. In particular, we will focus on the one-dimensional dynamics approach.

In his paper, Thurston studied unimodal maps, smooth functions with a unique critical point, an increasing branch, and a decreasing branch, via their semi-conjugacy with quadratic maps of the form $f(x) = ax^2 + bx + c$. The *Thurston Set* is the closure of all the Galois conjugates of the growth rates of unimodal maps that are critically periodic. The *growth rate* of a map is the value of the natural number e raised to the topological entropy of the map [Thu14], where entropy is a measure of the complexity of the dynamical system. In this paper, a tent map refers to a specific kind of piecewise linear function on the unit interval (see Definition 2.1). A tent map is critically periodic if the point 1 is strictly periodic, and β is critically periodic if its corresponding tent map, f_β, is critically periodic. Although tent maps

are not smooth, every unimodal map is semi-conjugate to a tent map with the same entropy, and the semi-conjugacy maps the critical point of the unimodal map to the peak $(\frac{1}{\beta}, 1)$ of the tent map. Therefore, the unimodal map is critically periodic if and only if the tent map is critically periodic. Because of the entropy preserving semi-conjugacy between quadratic maps and tent maps, it suffices to study the Thurston Set by investigating the tent maps [MT88].

Although semi-conjugacy can be entropy-decreasing, the semi-conjugacy between quadratic and tent maps preserves not only the entropy, but also itineraries. An itinerary is a sequence that describes the value of a mapping, $f(x)$, after each iteration [MT88]. Therefore, tent maps give us the minimal amount of information needed to understand the Thurston Set. Moreover, given an itinerary, it is always possible to reconstruct its tent map, yet reconstructing the quadratic map requires additional information.

Many researchers ([BDLW19], [CKW17], [Tho16], [Tio20]) have been inspired to study the Thurston Set. Some notable past results concern the bounds of the set. The Thurston Set has been proven to be path-connected and locally connected [Tio20]. It has been proven that all elements in the set have moduli greater than $\frac{1}{2}$ [Tio20], and the non-real elements in the set have moduli smaller than 1.6 [BBBP98]. There exist infinitely many holes in the fractal trees [CKW17]. The holes that lie on the the unit circle (Figure 1), however, are not actually holes and are filled in as the orbit length increases [Tio20]. Previous literature has explained why these particular gaps appear in plots of finite approximation of the Thurston Set [BDLW19]. Thurston's Master Teapot (Figure 4), in which the height of each element in the Thurston Set corresponds with its β value, grows monotonically with β [BDLW19].

The computation and visualization in this paper are made possible with the help of these results.

Remark 1.1 (On Figure 1)**.** Note that the points in Figure 1 were plotted in reverse orbit length order (i.e., points with higher orbit length were plotted before those with lower). Therefore, values with lower orbit length are marked on top of the preexisting values. If we had plotted from lowest orbit length to highest, the image would appear entirely pink as the number of critically periodic β values grows exponentially with the orbit length. Scripts for all the visualizations in this paper can be found here[2].

1.2. **Structure of the Paper.** This paper will walk through the creation of our data set and our key findings as follows:

> **Section 2,** Preliminaries: We provide background definitions of terminology important to generating the data set.
> **Section 3,** Storing the data of admissible strings: We describe our encoding algorithm and prove its viability.

[2] https://github.com/Tent-Maps-Team/Thurston-Set/tree/master/Visualizations/Scripts

Section 4, A list of combinatorial encodings for test: We combinatorically describe shifting for encoded itineraries.
Section 5, Testing admissibility of encodings: We prove an alternative admissibility criterion for encodings.
Section 6, Using the data: We show how we used the data set to better understand the distribution of critically periodic β, max-min values of the Thurston Set, and an analogy to the Mandelbrot-Julia Correspondence. We also make a conjecture about the largest real roots of Parry polynomials.
Section 7, Program time and space complexity: We investigate the worst-case time and space complexities of our script to generate the data set and show that the program must be slow.
Section 8, Entropy of the tent map: We prove directly that the entropy of the tent map of slope β is $\log \beta$.
Appendix A, Methodology: We discuss our code and our approach within Python to generate the data set.
Appendix B, Distribution of itineraries: A list of the number of itineraries in our data set for each orbit length from 3 to 33.
Appendix C, Additional visualizations from Subsection 6.4.3.
Appendix D, Additional details for the proofs in Section 8.

2. Preliminaries

2.1. **Basic definitions.** We will begin with the object of our study: the tent map.

Definition 2.1 (Tent map)**.** Denote the unit interval $[0, 1]$ by I. Fix a real number $\beta \in (1, 2]$. The *β-tent map* is the map $f_\beta : I \to I$ defined by

$$f_\beta(x) = \begin{cases} \beta x & \text{for } x \in [0, \frac{1}{\beta}) \\ 2 - \beta x & \text{for } x \in [\frac{1}{\beta}, 1]. \end{cases}$$

The function f_β is *critically periodic* provided that there exists some $n \in \mathbb{N}$ such that $f_\beta^n(1) = 1$. We call the corresponding β the *critically periodic β*, and the minimal such n the *orbit length* of f_β.

Definition 2.2 (Thurston Set [Thu14])**.** The *Thurston Set* is the closure of all of the Galois-conjugates for all critically periodic values of β.

Definition 2.3 (β-itinerary sequence)**.** A sequence, $(x_n) \in \{0, 1\}^{\mathbb{N}}$, is a *$\beta$-itinerary sequence* of a point $x \in I$ provided that $x_0 = 1$ and for $j > 0$,

$$x_j = \begin{cases} 0 & \text{if } f_\beta^j(x) \in [0, \frac{1}{\beta}) \\ 1 & \text{if } f_\beta^j(x) \in (\frac{1}{\beta}, 1], \end{cases}$$

for some value of $\beta \in (1, 2]$. If $f_\beta^j(x) = \frac{1}{\beta}$, then x_j can be either 0 or 1.

We notice that for all critically periodic values of β, there exists an associated itinerary sequence that is periodic with period n, the orbit length

defined above. A *word* is a finite string of characters, in our case, 0's and 1's. We say such a periodic itinerary sequence is *generated by* the word of length n that is repeated. Due to the semi-conjugacy between quadratic maps and tent maps, it is possible for a single β value to be represented by multiple itineraries. This manifests as ambiguity in in the value of a_j when $f_\beta^{j-1}(x) = \frac{1}{\beta}$. For a critically periodic β value, $f_\beta^n(1) = 1$, by definition. This means that $f_\beta^{n-1}(1) = \frac{1}{\beta}$ which can correspond to either a 1 or 0. So, a single critically periodic β value is associated with multiple itineraries. Note, the period of any periodic sequence associated with a certain β is an integer multiple of n, the orbit length of β.

Example 2.4. The following words generate some of the possible itineraries for the critically periodic β value φ, the Golden Ratio:

- $(1, 0, 1)$
- $(1, 0, 0)$
- $(1, 0, 1, 1, 0, 1)$
- $(1, 0, 0, 1, 0, 0)$
- $(1, 0, 0, 1, 0, 1)$

It is also possible that an itinerary sequence associated with β is not periodic. Consider

$$(1, 0, 1, 1, 0, 0, 1, 0, 1, 1, 0, 0, 1, 0, 0, 1, 0, 1, \dots).$$

To have an accurate idea of how many critically periodic values of β we have found and to maintain a clean data set, we want to associate a single itinerary with each critically periodic β value. To capture this one to one correspondence algorithmically, we must devise a system for removing duplicates. The justification for this system depends on a few more definitions.

Definition 2.5 (Cumulative sign sequence)**.** The *cumulative sign sequence* associated to a sequence $x = (x_0, x_1, \dots) \in \{0, 1\}^{\mathbb{N}}$ is defined by $S_0 = 1$ and for $j > 0$,

$$S_j = \begin{cases} 1 & \text{if } \sum_{k=0}^{j-1} x_k \text{ is even,} \\ -1 & \text{if } \sum_{k=0}^{j-1} x_k \text{ is odd.} \end{cases}$$

Furthermore, a word has *positive cumulative sign* if the sum of its entries is even, and *negative cumulative sign* if it's odd.

2.2. **Ordering and admissibility of itineraries.**

Definition 2.6 (Twisted lexicographical ordering [Par60])**.** Define the ordering $\leq_{\text{twist}}$ on the set of sequences in $\{0, 1\}^{\mathbb{N}}$ as follows. Let $x = (x_0, x_1, \dots)$ and $y = (y_0, y_1, \dots)$ be two distinct sequences in $\{0, 1\}^{\mathbb{N}}$.

We define $x <_{\text{twist}} y$ if and only if $x_0 < y_0$ or at the first integer $n > 0$ such that $x_n \neq y_n$,

$$\begin{cases} x_n < y_n & \text{if } \sum_{k=0}^{n-1} x_k \text{ is even,} \\ x_n > y_n & \text{if } \sum_{k=0}^{n-1} x_k \text{ is odd.} \end{cases}$$

Definition 2.7 (Admissible [MT88])**.** Let $x \in \{0,1\}^{\mathbb{N}}$ be an infinite periodic sequence, and denote $x = (x_0, \ldots, x_{n-1})$ where n is the period of the sequence. Let $\sigma : \{0,1\}^{\mathbb{N}} \to \{0,1\}^{\mathbb{N}}$ be the shift map on infinite periodic sequences such that $\sigma(x_0, x_1, x_2, \ldots, x_{n-1}) = (x_1, x_2, \ldots, x_{n-1}, x_0)$. We can define the string x to be *admissible* provided that it satisfies the following:

- $\sigma^i(x_0, \ldots, x_{n-1}) \leq_{\text{twist}} (x_0, \ldots, x_{n-1})$, for $i \in \{1, \ldots, n\}$,
- $\sum_{k=0}^{n-1} x_k$ is even. In other words, $(x_0, \ldots, x_{n-1})$ has positive cumulative sign.

Theorem 2.8 (Milnor-Thurston Admissibility Criterion [MT88])**.** *For any non-constant sequence $x \in \{0,1\}^{\mathbb{N}}$ that is minimal among the class of itineraries associated to a given β, there exists critically periodic $\beta \in (1,2]$ such that x is some β-itinerary if and only if x satisfies the admissibility criterion.*

Note that alone, the inequality condition in the admissibility criterion is not enough for the theorem. The positive cumulative sign property is often seen in the literature as minimality. We will make that connection explicit here.

We are now better able to consider redundant itineraries. Our computational methods for doing this are described in detail in Subsection 5.3. For each value of β, there exists a canonical choice of itinerary which we call the *minimal itinerary*. If we remove all non-minimal itineraries from our data set, we will have no redundant β values.

We consider a β-itinerary, It_β, to be *minimal* provided that It_β is admissible and is less than all the other possible admissible itineraries associated with that particular β according to the twisted lexicographical ordering described in Definition 2.6.

For example, in Example 2.4, the minimal itinerary for $\beta = \varphi$, the Golden Ratio, is $(1,0,1)$ because it is admissible, unlike $(1,0,0)$, and it is less than all other admissible strings according to the twisted lexicographical ordering. For this reason, $(1,0,1)$ is the itinerary we associate with $\beta = \varphi$ in our data set as we aim to include only minimal itineraries. Below, we provide criteria for identifying which itinerary is minimal.

Fact 2.9. *The minimal itinerary associated with a given value of β is generated by the word with minimal length and positive cumulative sign.*

Proof. Let x be a generating word with minimal length and positive cumulative sign. Since the cumulative sign is positive, we know that x has an

even number of 1's. Also, due to the nature of itinerary sequences, we know that a distinct itinerary sequence for the same β, generated by some $y \neq x$, can only differ from the itinerary generated by x in the $k(n-1)$-th position for some $k \in \mathbb{N}$, where n is the length of x.

Suppose the $k(n-1)$-th digit of x is 1. By assumption, this indicates that there are an odd number of 1's before this final entry. Since the $k(n-1)$-th digit of y must differ from x, we know y has a 0 in this position. Therefore, Definition 2.6 states that $x <_{\text{twist}} y$.

Now, suppose instead that the $k(n-1)$-th digit of x is 0. Then, our assumption tells us that there are an even number of 1's preceding this digit. Also, because the $k(n-1)$-th digit of y must differ from x, there is a 1 in the $k(n-1)$-th position of y. Thus, by Definition 2.6, $x <_{\text{twist}} y$.

Therefore, we have shown that the word with minimal length and positive cumulative sign generates the minimal itinerary for a given value of β. □

2.3. **Parry polynomials and their roots.** In order to approximate the Thurston set, we introduce Parry polynomials and β-conjugates below.

Definition 2.10 (Parry polynomial [Par60], [Par66])**.** For a periodic string x of length n with corresponding cumulative sign sequence $S = (S_0, \ldots, S_{n-1})$, the *Parry polynomial* is given by

$$P(z) = z^n - 2S_0x_0z^{n-1} - \cdots - 2S_{n-1}x_{n-1} - 1.$$

Definition 2.11 (β-conjugates [Par60], [Par66])**.** Fix a critically periodic value of β and say its minimal itinerary is generated by a string, x. Then, the roots of the Parry polynomial generated by x, including β itself, are *β-conjugates.*

Theorem 2.12 ([LW19])**.** *The Thurston Set intersected with $\mathbb{D}$ is the closure of all of the β-conjugates for all critically periodic values of β.*

Therefore, although not all β-conjugates are Galois conjugates, many β-conjugates are still in the Thurston Set. With this, we will be able to approximate the Thurston set by calculating the β-conjugate of all critical period values of β.

To further study the relationship between admissible itineraries and their associated critically periodic β, we attempt to calculate the value of β for all such itineraries with the help of Parry polynomials.

Fact 2.13 ([MT88])**.** *Let $P \in \mathbb{Z}[x]$ be a Parry polynomial for some string x that represents an itinerary of a critically periodic tent map, f_β. If $P/(z-1)$ is irreducible, then β is the largest real root of P.*

In other words, if P has only one real root in $(1, 2]$, then this root is the critically periodic β value associated with the polynomial. If P has more than one real root in $(1, 2]$, based on Conjecture 6.2, we propose to compute β by calculating the largest real root of the Parry polynomial.

3. Storing the Data of Admissible Strings

In compiling an extensive list of admissible strings, it benefits us to optimize our method of storing data. Our technique involves converting a series of arbitrary strings of 0's and 1's into *encoded strings* before deciding if they are admissible. By reducing the itineraries to encoded strings, we gain computational speed and memory efficiency. We store the data in a collection of .csv files dual-organized by orbit length and number of 1's in an admissible string. Each admissible string is stored in its encoded form, defined in Subsection 3.1, and paired with its orbit length.

Other mathematicians have produced images of the Thurston Set and Thurston's Master Teapot using strategies that have not been published, but have been shared by word-of-mouth. Our system of encoding was developed independently and differs slightly from the techniques created by other researchers.

In order to produce our data set, we first build a list of combinatorial encodings. As they are collected, we check the admissibility of the encoding, a step which requires a loop with length equal to the length of the combinatorial encoding. Next, if admissibility is satisfied, we check that the string is the shortest possible string to represent this value of β. If a string satisfies these conditions, we write the encoding and its orbit length to a .csv file.

3.1. Recording strings with encodings.

Naively, we could construct a list of all possible strings of 0's and 1's up to a certain length, test admissibility of these strings, and store only the admissible strings. However, we will much more efficiently be able to list combinatorial encodings and test their admissibility. Moreover, storing the encodings will take significantly less space.

To a string, $x = (x_0, \ldots, x_{n-1})$, of 0's and 1's, we associate an *encoded string*, $e = (e_0, \ldots, e_{k-1})$, where k is the number of 1's appearing in the string x, i.e. $k = \sum_{i=0}^{n-1} x_i$. We define e by only tracking the position of the 1's in the string x. More precisely, e_0 is the position of the first 1 to appear in the string x, and e_{j-1} is the position of the jth 1 to appear in the string x.

The mapping from strings to encodings will be denoted by E. Revisiting the notation above, that means $E(x) = e$. Notice that an encoding $E(x) = e$ is always increasing, is a substring of the increasing string $(0, \ldots, n-1)$, and $e_{k-1} \leq n-1$. The length of e is the number of 1's in a string, so for admissible strings, e must be even and must have length at least 2 and at most $n-1$, for odd n, or $n-2$, for even n.

Example 3.1. Consider the string (1, 0, 0, 1, 1, 1, 1, 0, 0, 1, 0, 0) of length 12. We encode this string as (0, 3, 4, 5, 6, 9) $n = 12$, storing the locations of the 1's.

We will define a *combinatorial encoding string* to be any monotonically increasing string of nonnegative integers.

Lemma 3.2. *For fixed n, there is a bijection between combinatorial encodings with length n and last term at most $n-1$ and strings of 0's and 1's of length equal to n.*

Proof. Let $x = (x_0, \ldots, x_{n-1})$ and $y = (y_0, \ldots, y_{n-1})$ be two strings of 0's and 1's such that $x \neq y$. Then, there exists $i \in \{0, \ldots, n-1\}$ such that $x_i \neq y_i$. Without loss of generality, let $x_i = 1$ and $y_i = 0$. By the definition of the map E, i is a term in the combinatorial sequence $E(x)$, yet not in $E(y)$. Thus, $E(x) \neq E(y)$ and E is injective. For any combinatorial encoding $e = (e_0, \ldots, e_{k-1})$ where $k < n$, there exists $x = (x_0, \ldots, x_{n-1})$ with $x_i = 1$ if and only if i is a term in e. Then, we have $E(x) = e$. Therefore, E is surjective and the bijection holds. □

4. A List of Combinatorial Encodings for Testing

The computational tool for developing a list of combinatorial encodings will be Python's itertools package. For more, see Appendix A.

Lemma 4.1. *For $n \geq 4$, there are*

$$\begin{cases} \sum_{j=0}^{(n-4)/2} \binom{n-2}{2j+1} & \text{if } n \text{ is even, and} \\ \sum_{j=0}^{(n-3)/2} \binom{n-2}{2j+1} & \text{if } n \text{ is odd} \end{cases}$$

many strings of 0's and 1's with an even number of 1's, length equal to n, and first two terms equal to 1 and 0.

Proof. Let $x = (x_0, \ldots, x_{n-1})$ be a string of length $n \geq 4$ satisfying the conditions of the lemma. Note that $x_0 = 1$ and $x_1 = 0$ is given. Consider the remaining $n-2$ entries of x, call this string, $(x_2, \ldots, x_{n-1})$, the *tail* of x. By the assumption that x has an even number of 1's, we know there are an odd number of 1's which we should position on this tail. Denote $k = 2j+1$ to be the number of 1's which we position in the tail for some non-negative integer j such that $k \leq n-2$. Loop through all values of k, and notice that we simply want $k = 2j+1 \leq n-2$ as we removed the x_0 and x_1 terms. Therefore, we have that $j \leq \frac{n-3}{2}$, and since j is an non-negative integer, $j \leq \lfloor \frac{n-3}{2} \rfloor$. Fix k as the number of 1's appearing in the tail of x (of length $n-2$). Then, there are $\binom{n-2}{k}$ many possible positions for a 1 in the tail. The conclusion follows. □

Example 4.2. Here is a list of the combinatorial encodings of all $\binom{7-2}{3} = 10$ strings of length 7 with 4 many 1's which begin with $(1, 0, \ldots)$:

$$(0,2,3,4), (0,2,3,5), (0,2,3,6), (0,2,4,5), (0,2,4,6),$$

$$(0,2,5,6), (0,3,4,5), (0,3,4,6), (0,3,5,6), (0,4,5,6).$$

5. Testing Admissibility of Encodings

Let $e = E(x)$ be an encoding of a string $x = (x_0, \ldots, x_{n-1})$ of length n with an even number of 1's. We wish to determine admissibility of x via the data of e. To do this, we will need the induced action of the shift on encodings and the induced Milnor-Thurston admissibility criterion for encodings.

5.1. **Shifting an encoding string.** We define a modified shift, $\underline{\sigma}$, on an encoding, e; that is, if $e = (e_0, \ldots, e_{k-1})$ and $e_0 = 0$, then $\underline{\sigma}(e) = (e_1 - e_1, \ldots, e_{k-1} - e_1, n - e_1) = (0, \ldots, e_{k-1} - e_1, n - e_1)$.

Lemma 5.1. *Let x be any string with initial term equal to 1, and $E(x) = (e_0, \ldots, e_k)$. Then,*

$$\underline{\sigma}(E(x)) = E(\sigma^{e_1}(x)).$$

Proof. Let $x = (x_0, \ldots, x_{n-1})$, and $x_i = 1$ if and only if $i \in \{e_0, \ldots, e_{k-1}\}$. Since $x_0 = 1$, we see,

$$\begin{aligned} E(\sigma^{e_1}(x)) &= E((x_{e_1}, x_{e_1+1}, \ldots, x_{n-1}, x_0, \ldots, x_{e_1-1})) \\ &= (0, \ldots, e_{k-1} - e_1, n - e_1) \\ &= \underline{\sigma}(E(x)). \end{aligned}$$

□

5.2. **An admissibility criterion for encodings.** To introduce the induced Milnor-Thurston admissibility criterion for combinatorial encodings we will need an induced twisted lexicographical ordering. We define the modified twisted lexicographical ordering, $>_{\underline{\text{twist}}}$, on an encoding, e, in the following way.

Let $e = (e_0, \ldots, e_{k-1})$ and $f = (f_0, \ldots, f_{k-1})$ be combinatorial encodings of the same length k. Then, $e <_{\underline{\text{twist}}} f$ if and only if at the first index i in $(0, \ldots, k-1)$ at which the terms of e and f differ,

$$\begin{cases} e_i < f_i & \text{if } i \text{ is odd, or} \\ e_i > f_i & \text{if } i \text{ is even.} \end{cases}$$

Proposition 5.2. *If x and y are strings of 0's and 1's, each with initial term equal to 1, of the same length and containing the same total number of 1's, then the encoding map will preserve the twisted lexicographical ordering between x and y. That is:*

$$x <_{\text{twist}} y \iff E(x) <_{\underline{\text{twist}}} E(y).$$

Proof. First, we will show the forward direction. Let x and y have length n and suppose $x <_{\text{twist}} y$. Then, there exists $i \in \{0, \ldots, n-1\}$ where i is the least integer such that $x_i \neq y_i$. Denote $S_i = \sum_{m=0}^{i-1} x_m = \sum_{m=0}^{i-1} y_m$. So, by definition, we know either

(I) $x_i > y_i$ and S_i is odd, or

(II) $x_i < y_i$ and S_i is even.

Since x and y have an equal number of 1's in total, we know $E(x)$ and $E(y)$ are of the same length. Call this length k. Let $E(x) = e = (e_0, \ldots, e_{k-1})$, and $E(y) = f = (f_0, \ldots, f_{k-1})$.

Consider case (I). In this case, we have $x_i = 1$ and $y_i = 0$. Let x_i correspond to e_j in e, meaning $e_j = i$. As S_i is odd, there must be an odd number of 1's before x_i which implies j is odd. Because $y_i = 0$, we also know $f_j \neq e_j$. In fact, the next 1 in y must come later in the sequence, so $e_j < f_j$. Therefore, $e <_{\underline{twist}} f$.

Now, consider instead case (II). In this case, we have $x_i = 0$ and $y_i = 1$. Let y_i correspond to f_j in f, meaning $f_j = i$. We know there are an even number of 1's before y_i because S_i is even. Thus, j must be even. Also, since $x_i = 0$, we see $e_j \neq f_j$, so the jth 1 in x must come later in the sequence. Therefore, $e_j > f_j$ which implies $e <_{\underline{\text{twist}}} f$.

Therefore, $x <_{\text{twist}} y$ implies $E(x) <_{\underline{\text{twist}}} E(y)$.

Now, let's show the reverse direction. Let $e = E(x) = (e_0, \ldots, e_{k-1})$ and $f = E(y) = (f_0, \ldots, f_{k-1})$ encode two strings x and y, each with length n. Suppose $e <_{\underline{\text{twist}}} f$. Then, we know that for some natural number $i \in \{0, \ldots, k-1\}$ either,

(i) $e_j < f_j$ and j is odd, or

(ii) $e_j > f_j$ and j is even,

where j is the least integer such that $e_j \neq f_j$.

Consider case (i). Let x_i correspond with e_j, meaning $i = e_j$. Since j is odd, we know there are an odd number of 1's that precede x_i. Also, because $e_j < f_j$, we know $x_i = 1$ while $y_i = 0$. Thus, $x_i > y_i$ and $S_i = \sum_{m=0}^{i-1} x_m = \sum_{m=0}^{i-1} y_m$ is odd. So, (i) implies $x <_{\text{twist}} y$.

Now, consider case (ii). Again, let x_i correspond with e_j so $i = e_j$. Since j is even, we know there are an even number of 1's that precede x_i. Additionally, because $e_j > f_j$, we know $x_i = 0$ while $y_i = 1$. Therefore, $S_i = \sum_{m=0}^{i-1} x_m = \sum_{m=0}^{i-1} y_m$ is even and $x_i < y_i$. So, (ii) implies $x <_{\text{twist}} y$.

Hence, $E(x) <_{\underline{\text{twist}}} E(y)$ implies $x <_{\text{twist}} y$.

Therefore, $x <_{\text{twist}} y$ if and only if $E(x) <_{\underline{\text{twist}}} E(y)$.

□

We define a combinatorial encoding, e, to be an *admissible encoding* if there exists an admissible string x such that e is the encoding of x. Now we are ready to state the induced Milnor-Thurston admissibility criterion on encodings.

Theorem 5.3. *Let $e = (e_0, \ldots, e_{k-1})$ be a combinatorial encoding. Then e is an admissible encoding if and only if for all $i \in \{0, \ldots, k-1\}$,*

$$\underline{\sigma}^i(e) \leq_{\underline{\text{twist}}} e.$$

Proof. We prove this theorem by contrapositive. We will show that e is not an admissible encoding if and only if there exists some $i \in \{0, \ldots, k-1\}$

such that $\underline{\sigma}^i(e) >_{\underline{\text{twist}}} e$. Suppose there exists an $i \in \{0, \ldots, k-1\}$ such that $\underline{\sigma}^i(e) >_{\underline{\text{twist}}} e$ for a string x and its encoding, $e = E(x)$. We see $\underline{\sigma}^i(e) >_{\underline{\text{twist}}} e$ is equivalent to $\underline{\sigma}^i(E(x)) >_{\underline{\text{twist}}} E(x)$. Then, by Lemma 5.1 and Proposition 5.2,

$$E^{-1}\underline{\sigma}^i(E(x)) = \sigma^{e_i}(x) >_{\text{twist}} x = E^{-1}(E(x)).$$

Consider $\sigma^\alpha(x)$ where $\alpha = e_i$. Then, from above, we know $\sigma^\alpha(x) >_{\text{twist}} x$ so x is not an admissible string.

Suppose e is not an admissible encoding. Then, x is not an admissible string. So, for some α, we have $\sigma^\alpha(x) >_{\text{twist}} x$. We claim that $\alpha = e_i$ for some $i \in \{0, \ldots, k-1\}$. If this is not the case, then, by definition of e_i, $\sigma^\alpha(x)$ begins with a 0 while x begins with a 1. Therefore, $\sigma^\alpha(x) <_{\text{twist}} x$, which contradicts our assumption. So, it must be that $\alpha = e_i$ for some $i \in \{0, \ldots, k-1\}$. Hence, the remaining implications mirror the reverse direction.

Therefore, e is not an admissible encoding if and only if there exists some $i \in \{0, \ldots, k-1\}$ such that $\underline{\sigma}^i(e) >_{\underline{\text{twist}}} e$. Thus, e is an admissible encoding if and only if for all $i \in \{0, \ldots, k-1\}$, $\underline{\sigma}^i(e) \leq_{\underline{\text{twist}}} e$. □

5.3. **Checking irreducibility.** When compiling this data set, we aimed to ensure that each itinerary corresponds to a unique value of β. Therefore, the number of itineraries is equal to the number of critically periodic β values up to a given orbit length. There are two potential types of redundancy within our data set, and we eliminated the first type of the redundancy introduced in the following.

5.3.1. *Periodicity.* The first type of redundancy is due to periodicity. Since the itineraries of critically periodic β are periodic, it is necessary to reduce each sequence to its shortest unrepeated subsequence. For example, consider the two strings $(1, 0, 1)$ and $(1, 0, 1, 1, 0, 1)$. We notice that when repeated infinitely these two finite strings form the same sequence. Therefore, the two strings represent itineraries of the same β value and including both in our data set would be redundant. We call the former sequence *irreducible* because it is the shortest possible string to represent this value of β.

We check for irreducibility through shifting. A string x of length n is *reducible* provided that there exists a natural number $m < n$ such that $\sigma^m(x) = x$. In the case of our example, $x = (1, 0, 1, 1, 0, 1)$, we see $\sigma^3(x) = x$ and $3 < n = 6$. Therefore, x is reducible.

The process for checking irreducibility of encodings is similar to that for unencoded strings. We again employ a shifting technique, using the shift for encodings described in Lemma 5.1 and the length of the encoding instead of the standard shift and the orbit length. More precisely, an encoded string $E(x)$ of length $k \leq n$, where n is the orbit length of x, is reducible provided that there exists a natural number $j < k$ such that $\underline{\sigma}^j(E(x)) = E(x)$.

Proposition 5.4. *A string x is reducible if and only if its encoding $E(x)$ is reducible.*

Proof. First, suppose x is a reducible string of orbit length n. Then, there exists a natural number $m < n$ such that $\sigma^m(x) = x$. Since the two strings are equal, their encodings are as well. Denote $E(x)$ as $e = (e_0, \ldots, e_k)$. Also, we know that $x_0 = x_m = 1$. Therefore, for some natural number $j < k$, x_m corresponds with e_j, meaning x_m is the jth 1 in the string and $e_j = m$. So,

$$E(x) = E(\sigma^m(x)) = E(\sigma^{e_j}(x)) = \underline{\sigma}^j(E(x)).$$

Thus, $E(x)$ is also reducible.

Now, instead suppose that $E(x) = e = (e_0, \ldots, e_k)$ is reducible. Then, by definition, there exists a natural number $j < k$ such that $\underline{\sigma}^j(E(x)) = E(x)$. Therefore, by Lemma 5.1,

$$E(x) = \underline{\sigma}^j(E(x)) = E(\sigma^{e_j}(x)).$$

Since the encodings of the two strings are equal, the strings themselves are also equal. Thus, $m = e_j < n$ and we see x is also reducible.

Hence, a string x is reducible if and only if its encoding $E(x)$ is reducible. □

Example 5.5. Consider the example provided above, $x = (1, 0, 1, 1, 0, 1)$. As suggested earlier, this string is reducible to $(1, 0, 1)$. Let's examine $E(x)$ to determine that x is indeed reducible.

We can encode x as $E(x) = (0, 2, 3, 5)$. Then, using the process described above, we have $k = 4$ and,

$$\underline{\sigma}(E(x)) = (0, 1, 3, 4)$$
$$\underline{\sigma}^2(E(x)) = (0, 2, 3, 5) = E(x).$$

Since $\underline{\sigma}^2(E(x)) = E(x)$ and $2 < k = 4$, we see that $E(x)$, and therefore x, is reducible.

Due to our thorough process for checking irreducibility, we are able to remove all duplicates of this type from our data set.

5.3.2. *Boundary choice.* The second type of redundancy arises due to the ambiguity in choosing the final element of a string as alluded to in Section 2: Preliminaries. When $f_\beta^{j-1}(x) = \frac{1}{\beta}$, we have a choice of 0 or 1 as the jth term in our itinerary string. If this type of duplicate is admissible, our code will not be able to eliminate them due to computational reasons. Still taking the Golden ratio as an example, our code will note be able to eliminate itinerary $(1, 0, 1, 1, 0, 0, 1, 0, 0)$.

When rounded to 13 decimal places of precision and considering all critically periodic β values with orbit length $n \leq 30$, we find 286 possible duplicates out of 37,123,039 itineraries, about 0.00077%. Due to rounding, this number acts as an upper bound of the actual amount of repeats in our data set. Considering the computational difficulty of completely removing these redundant itineraries, we opted to leave the small proportion in the set.

6. Using the Data: A Collection of Examples

6.1. **A histogram of growth rates of critically periodic tent maps.** Below are two distribution plots made using the data set. From the set of itineraries, we are able to calculate the associated critically periodic values of β and their orbit lengths by creating Parry polynomials and taking their roots. This gives us the information necessary to make these plots.

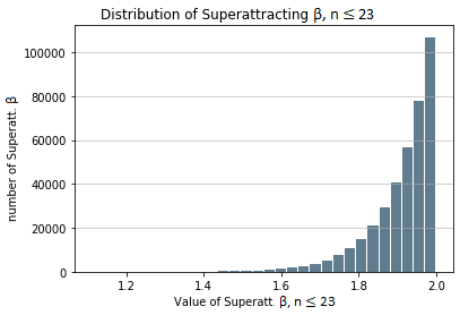

FIGURE 2. The distribution of critically periodic β in $(1, 2]$.

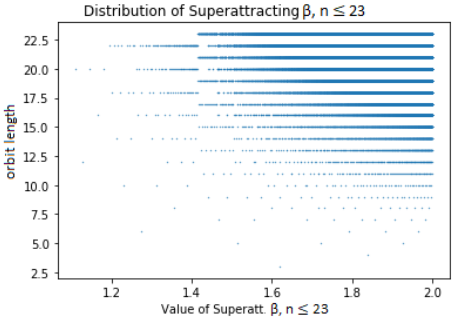

FIGURE 3. The relationship between orbit length and β.

Before describing the plots in detail, we must introduce the concept of period-doubling.

Definition 6.1 (Period-doubling [BDLW19])**.** If β is critically periodic with orbit length n, then $\sqrt{\beta}$ is also critically periodic with orbit length $2n$. We call this phenomenon *period-doubling*.

In the histogram (Figure 2), we see the number of critically periodic β values appears to increase exponentially as we increase the value of β. Because we collected the data by finding itineraries instead of β values directly, we know that all possible critically periodic β with orbit length $n \leq 23$ are included. However, Tiozzo states that there are an infinite amount of critically periodic β values in all value ranges [Tio20]. This leads us to believe that the exponential behavior arises from our arbitrary limit on the orbit length and, in reality, the density could be uniform. The exponential nature of period-doubling causes the lower values to fill in more slowly: many lower β values have a longer orbit length. So, asymptotically with respect to the period length n, the graph of the density is likely not exponential as a function of β.

On the right (Figure 3), we plot the value of β against its orbit length. This image also reveals some interesting consequences of period-doubling. For example, this behavior creates a lower bound of $\sqrt{2}$ on critically periodic β values with odd orbit length. For any $\beta \leq \sqrt{2}$ with orbit length n, $\beta^2 \in (1, 2]$, is also critically periodic, and would have orbit length $\frac{n}{2}$. However,

for an odd orbit length, $\frac{n}{2}$ is not a whole number so this is impossible. In addition, for any $\beta \leq \sqrt{2}$ with even orbit length, we know β^2 is also included in the scatterplot, with half the orbit length.

6.2. **The Thurston Set and the Thurston Master Teapot.** Another use of our data set is to generate detailed approximations of the Thurston Set (Figure 1) and Thurston's Master Teapot (Figure 4). The image of the Thurston Set and Thurston Master's Teapot include 8,384,382 points up to orbit length 23 and 1,046,463 points up to orbit length 20, respectively.

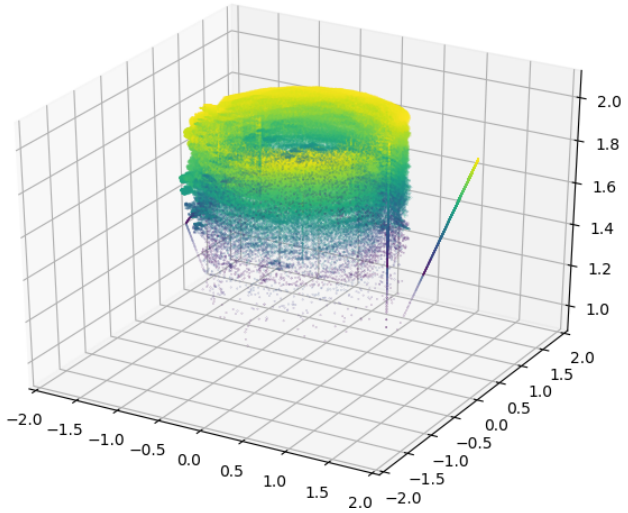

FIGURE 4. Approximation of Thurston Master Teapot.

To turn the list of encoded itineraries into a collection of points, we first transform the encoded itineraries into Parry polynomials. Then, we use the Python package NumPy to find the roots of each Parry polynomial.

For Parry polynomials with only one real root in $(1, 2]$, according to Fact 2.13, this real root is the critically periodic β. For itineraries with orbits less than or equal to 23, about 8% of the 269,017,181 itineraries have multiple real roots. Experimentally, for all of these Parry polynomials that have multiple real roots in $(1, 2]$, its largest real root is always the critically periodic β associated with the itinerary. Based on the results of this experiment[3], we propose the following conjecture.

Conjecture 6.2. *If $P \in \mathbb{Z}[x]$ is a Parry polynomial for some string x that represents an itinerary of a critically periodic tent map, f_β, then β is the largest real root of P.*

Based on this conjecture, we created an animation of Thurston's Master Teapot that shows how the β-conjugates accumulate as we increase orbit

[3]`https://github.com/Tent-Maps-Team/Thurston-Set/tree/master/Conjecture`

length. The completed Teapot is shown above in Figure 4. This animation revealed that the bottom of the Master Teapot is filled up more slowly than the top. As described in Subsection 6.1, critically periodic β with values near 2 have shorter orbit length than those less than $\sqrt{2}$ due to period-doubling. This phenomenon makes it difficult to plot the Master Teapot with β values of the plotted points that are roughly uniformly distributed with respect to height because exponentially more points are needed to find values of β in $(1, \sqrt{2})$.

In the approximation of the Thurston Set, we colored-coded each point according to its orbit length (Figure 1). This image shows a large number of points with different orbit length are distributed around the unit circle, implying that the values near the unit circle are very common β-conjugates for β of any orbit length. This coloring revealed that there are many holes on the unit circle (which are proved to be "fake" holes that get filled in as the orbit length increases [Tio20], [BDLW19]), and that points involved in the fractal behavior appear most slowly.

Generating such detailed images allowed us to zoom in on the Thurston Set and investigate its properties, such as an analogy to the Mandlebrot-Julia correspondence [Lei90a].

6.3. **The upper and lower bounds of moduli of the elements in the Thurston Set.** In previous literature, it has been proven that the non-real elements in the Thurston Set have moduli bounded above by 1.6 [BBBP98], and all the elements are bounded below by 0.5 [Tio20].

We plot the maximum and minimum moduli of elements in the Thurston Set against orbit length in order to visualize the bounds of the non-real elements and to compare our experimental bounds with those given in the literature. Figure 5 shows that the maximum and the minimum moduli seem to converge as orbit length increases.

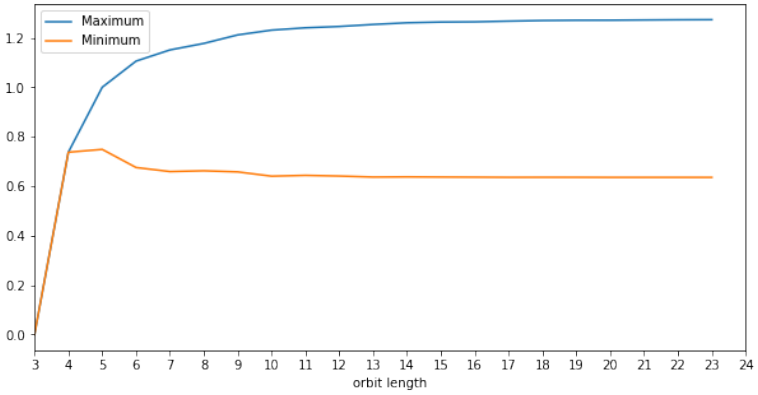

FIGURE 5. The maximum and the minimum moduli.

To study the convergence of the maximum and minimum moduli, we calculate the ratio between the maximum moduli points in the Thurston set corresponding to periodic orbits of length n n and $n-1$ as well as the ratio between the minimum moduli points in the Thurston set corresponding to periodic orbits of lengths n and $n-1$ and plot these ratios with respect to n. As these ratios appear to converge to 1 (Figure 6), we conjecture that both the maximum and the minimum moduli converge with respect to the orbit length. Data up to orbit length 23 suggest that the maximum modulus approaches $1.2733506936267585 < 1.6$, while the minimum modulus approaches $0.6356448144210942 > 0.5$.

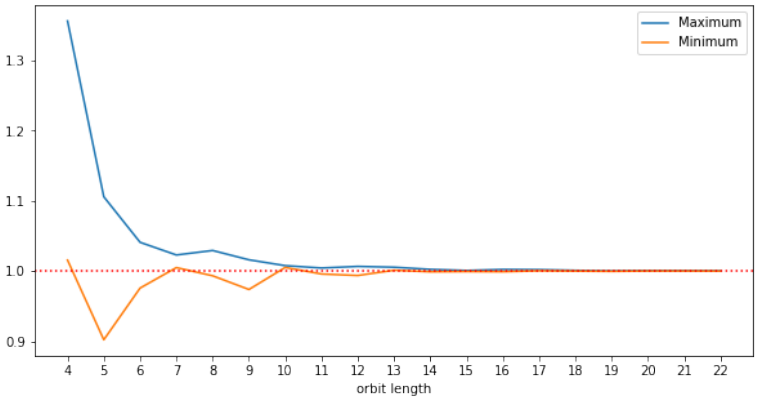

FIGURE 6. Ratios of maximum and minimum moduli.

Below, Figure 7 superimposes green and orange circles over the Thurston Set to visualize the maximum and minimum moduli for various orbit lengths.

6.4. **An analogy to the Mandlebrot-Julia Correspondence.** Inspired by a question posed by Lindsey and Wu, we investigate a correspondence between the Thurston Set and its attracting sets that is analogous to the Mandelbrot-Julia Correspondence [Lei90b]. Intuitively, this correspondence suggests that an attracting set resembles the local behavior of a subset of the Thurston Set.

6.4.1. *Analogy to the Mandelbrot Set.* Previous research ([CKW17], [LW19]) shows that, for the analogy to the Mandelbrot Set, we should consider the subset of the Thurston Set which is the horizontal "slice" of Thurston's Master Teapot at some fixed height β. We denote the closure of this subset as Υ_β. Let $\mathbb{D}$ be the subset of the complex plane within the unit disk, and let $\Upsilon_\beta^{\mathbb{D}}$ be the candidate of the analogy to the Mandelbrot Set, where

$$\Upsilon_\beta^{\mathbb{D}} = \mathbb{D} \cap \Upsilon_\beta = \mathbb{D} \cap \overline{\{z \in \mathbb{C} : z \text{ is a } \beta\text{-conjugate}\}}.$$

Note that the subset of the Thurston Set we choose as our candidate depends on the value of β. As such, a different choice of β could produce a

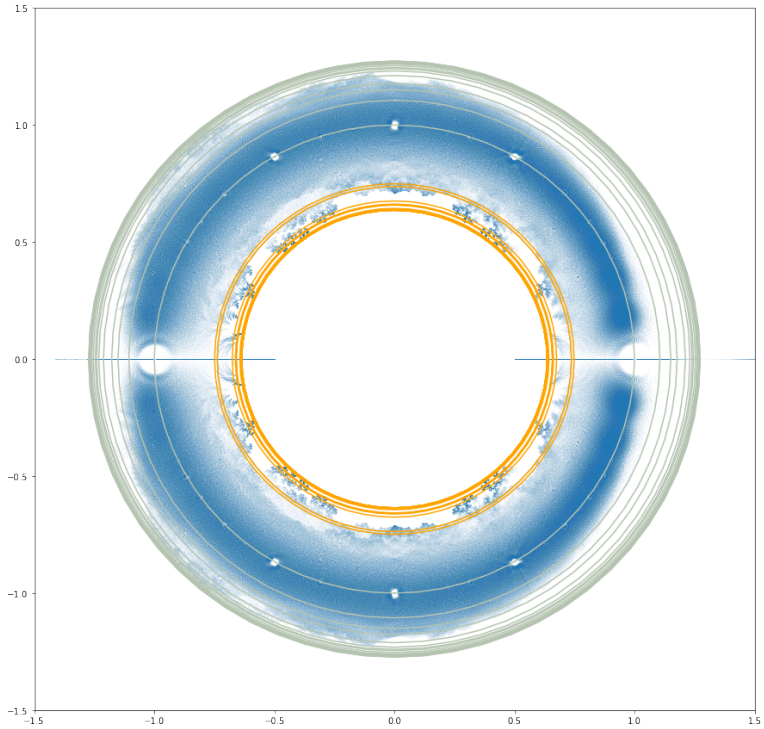

FIGURE 7. The maximum and the minimum moduli for various orbit lengths.

different set. In order to approximate $\Upsilon_\beta^{\mathbb{D}}$, we must utilize the Persistence Theorem [BDLW19].

Theorem 6.3 (Persistence [BDLW19, Theorem 1])**.** *For some $\beta \in (1,2]$, fix $z \in \Upsilon_\beta^{\mathbb{D}}$. Then, for any $\beta' \in [\beta, 2]$, $z \in \Upsilon_{\beta'}^{\mathbb{D}}$.*

Theorem 6.3 implies that, for a fixed β', an approximation of $\Upsilon_{\beta'}^{\mathbb{D}}$ can be obtained by plotting the β-conjugates for all $\beta < \beta'$ in the complex plane. Next, we will consider the Julia Set.

6.4.2. *Analogy to the Julia Set.* As done in previous literature ([CKW17], [LW19]), we construct the analogy to the Julia Set using the following restricted iterated function system (IFS).

Denote $It_\beta(1,\cdot)$ as the minimal β-itinerary sequence of 1, as defined in Fact 2.9. Let $\mathscr{A}_\beta$ be the set of all sequences in $\{0,1\}^{\mathbb{N}}$ that are less than or equal to $It_\beta(1,\cdot)$:

$$\mathscr{A}_\beta := \{a_\infty \in \{0,1\}^\infty : a_\infty \leq_{\text{twist}} It_\beta(1,\cdot)\}.$$

Fix β and $c \in \Upsilon_\beta^{\mathbb{D}}$. Define a IFS with the contracting map

$$\begin{cases} f_{0,c}(z) = c \cdot z \\ f_{1,c}(z) = 2 - c \cdot z. \end{cases}$$

Define the function g over $\mathscr{A}_\beta$ such that for any $a_\infty \in \mathscr{A}_\beta$,

$$a_\infty \mapsto (f_{a_1,c}(1), f_{a_2,c}(1) \circ f_{a_1,c}(1), f_{a_3,c}(1) \circ f_{a_2,c(1)} \circ f_{a_1,c}(1), \dots),$$

where a_n refers to the nth element in the sequence a_∞. We denote the set of accumulation points of every element in the image of g as $\bigwedge_{\beta,c}$ and choose it as our analogy to the Julia Set. Note that this method is a restriction of the IFS to the sequences in $\mathscr{A}_\beta$. Due to the Persistence Theorem (Theorem 6.3), the true IFS (the system in which all sequences are allowed) corresponds to the intersection of $\mathbb{D}$ and the Thurston set.

Since it can be time consuming to list all the sequences less than a given $It_\beta(1, \cdot)$, to visualize an approximation of $\bigwedge_{\beta,c}$, we simplify this procedure by fixing a critically periodic β and search for all sequences less than $It_\beta(1, \cdot)$ to the search for all cyclic sequences that

(1) are less than $It_\beta(1, \cdot)$ and
(2) have cycle length equal to the orbit length of β.

6.4.3. *Visualization.* If the Thurston Set and its attractors are indeed analogous to the Mandlebrot-Julia correspondence, we expect to see that the attractor $\bigwedge_{\beta,c}$ resembles the local behavior around c of the "slice" of Thurston's Master Teapot (Figure 8) at height β.

To empirically test the correspondence between $\Upsilon_\beta^{\mathbb{D}}$ and $\bigwedge_{\beta,c}$, we first fix the parameter c to observe the change of $\Upsilon_\beta^{\mathbb{D}}$ and $\bigwedge_{\beta,c}$ as the height β varies, and then fix the height β to observe the change of the two sets as the parameter c varies.

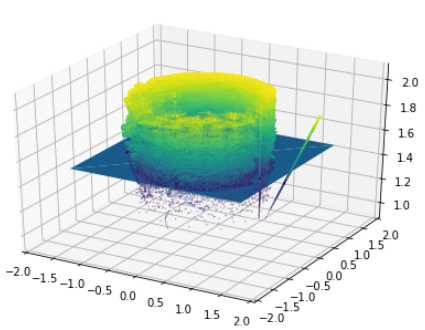

Thurston's Master Teapot at height $\beta = 1.5137084752402$

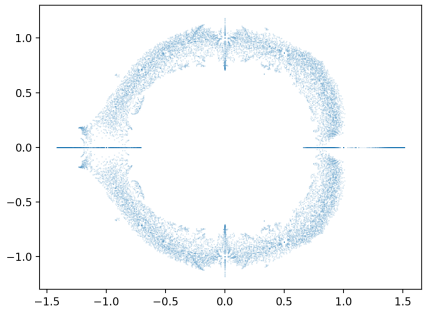

"Slice" of Thurston's Master Teapot at height $\beta = 1.5137084752402$

FIGURE 8. Analogy to Mandelbrot Set.

To visualize the change of the two sets as β varies, we fix

$$c_0 = 0.282888173224922 + 0.645528282687951i.$$

Note, c_0 is a β-conjugate for the critically periodic

$$\beta_0 = 1.5137084752402,$$

which has orbit length $n = 22$ and encoded sequence

$$e_{\beta_0} = (0, 2, 3, 5, 7, 8, 9, 10, 12, 13, 14, 15, 17, 19, 20, 21).$$

Since $|c_0| = 0.7048 < 1$, we know $c_0 \in \Upsilon^{\mathbb{D}}_{\beta_0}$. Let

$$\beta_1 = 1.97780753328 \text{ and } \beta_2 = 1.9980436378746.$$

Note that β_1 and β_2 are both critically periodic with orbit length $n = 22$. By the Persistence Theorem (Theorem 6.3), $c_0 \in \Upsilon^{\mathbb{D}}_{\beta_1}$ and $c_0 \in \Upsilon^{\mathbb{D}}_{\beta_2}$.

If an analogous Mandelbrot-Julia correspondence exists, we expect $\bigwedge_{\beta_0,c_0}$, $\bigwedge_{\beta_1,c_0}$, and $\bigwedge_{\beta_2,c_0}$ to resemble the local behavior of $\Upsilon^{\mathbb{D}}_{\beta_0}$, $\Upsilon^{\mathbb{D}}_{\beta_1}$, and $\Upsilon^{\mathbb{D}}_{\beta_2}$ at c_0, respectively. In Figure 9, the red dot represents the position of c_0. It can be seen from the three graphs on the left that, as β increases, the sets of accumulation points at c_0 becomes denser. Though not as obvious, in the three graphs on the right, the attractor at c_0 becomes more concrete as β increases. This supports the conjectured analogy to the Mandelbrot-Julia correspondence.

As the height β increases, the "slice" of Thurston's Master Teapot, Υ_β, at c_0 becomes denser and the fractal $\bigwedge_{\beta,c}$ grows more complete. Note that because our approximation of Thurston's Master Teapot contains only data up to orbit length $n = 23$, the change between images of Υ_β at c_0 appears to be much more dramatic than in the attractors.

To visualize the change in the two sets as the parameter c is varied, we fix $\beta_3 = 1.9980436378746$, and let

$$\begin{array}{lll} c_1 = -0.67 + 0.1i & c_2 = 0.59 + 0.26i & c_3 = 0.75i \\ c_4 = 0.61 + 0.3i & c_5 = 0.707 + 0.707i & c_6 = 0.71 + 0.71i \\ c_7 = -0.45 + 0.5i & c_8 = -0.4 + 0.45i. & \end{array}$$

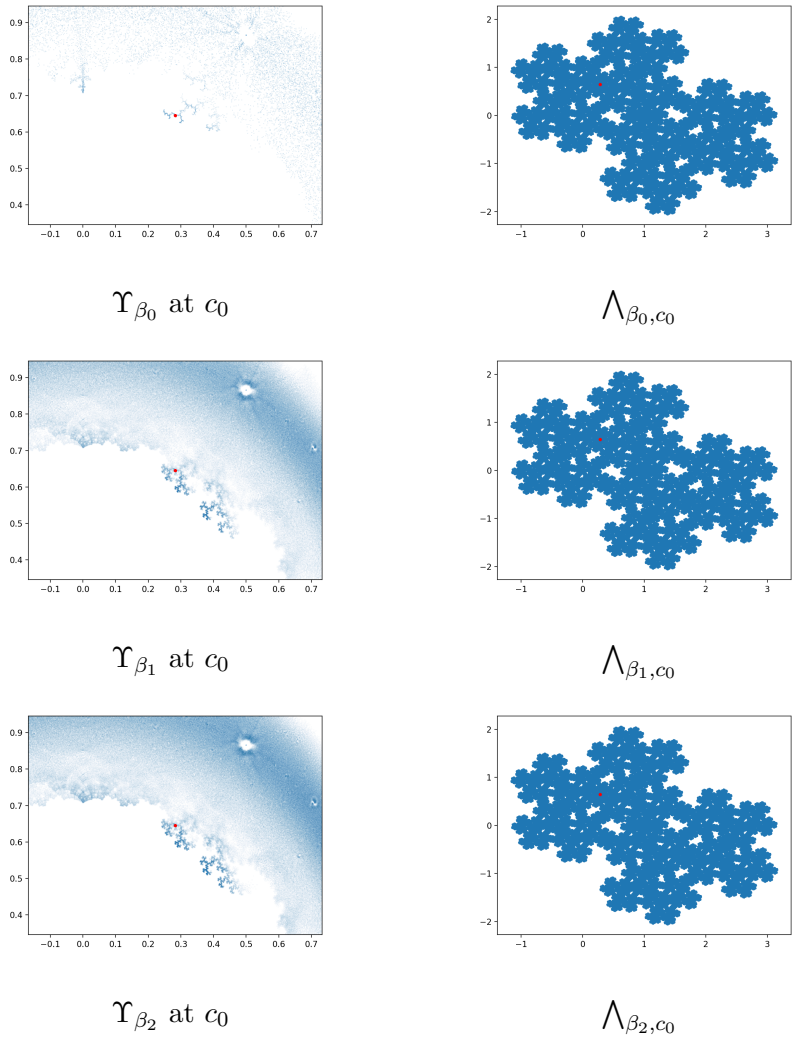

FIGURE 9. Varied values of β with constant c.

To study the behavior of $\bigwedge_{\beta,c}$ and Υ_β near the boundary of Υ_β, we compare their approximations centered at $c = c_1, c_2, c_3, c_4$. As shown in Figure 10 (see Appendix C), $\bigwedge_{\beta,c}$ resembles the local behavior of Υ_β as c varies, supporting the existence of an analogous Mandelbrot-Julia Correspondence.

The approximations of $\bigwedge_{\beta,c}$ and Υ_β centered at $c = c_5, c_6$ allow us to study the behavior of the sets near the roots of unity. As shown in Figure 11 (see Appendix C), small variation in c can result in a drastic change in the attractor, $\bigwedge_{\beta,c}$, just as is the case with the Mandelbrot and Julia Sets.

To understand the behavior of $\bigwedge_{\beta,c}$ and Υ_β for c inside and outside of Υ_β, we compare their approximations centered at $c = c_7$ and c_8. As shown in Figure 12 (see Appendix C) in conjunction with Figures 9, 10, and 11,

the point c is an element of Υ_β if and only if the fractal attractor, $\bigwedge_{\beta,c}$, is connected. This is consistent with the Mandelbrot-Julia Correspondence.

Overall, our calculations and visualizations have given encouraging evidence in support of an analogous Mandelbrot-Julia Correspondence. Further investigation is necessary to prove such an analogy exists.

7. Program Time and Space Complexity

We will now analyze the program time and space complexity of our algorithms to show that our solution is nearly optimal but ultimately (and inescapably) slow due to our vast search space. To generate all admissible itineraries of length n, we first generate all encoded strings representing itineraries of length n with an even number of 1's, then check if each encoded itinerary is admissible.

We can quantify the number of candidate itineraries generated using Lemma 4.1. Since there is a bijection between each itinerary and its encoding, as shown in Lemma 3.2, the number of length n itineraries with an even number of 1's and the number of encodings that represent such an itinerary are equal. Python's itertools[4] efficiently generates these $\sum_{j=0}^{(n-4)/2} \binom{n-2}{2j+1}$ or $\sum_{j=0}^{(n-3)/2} \binom{n-2}{2j+1}$ combinations.

For each of these encoded candidate itineraries, we check admissibility using the test found in Theorem 5.3. Given an encoded itinerary of length n, we check that the inequality holds for all $n-1$ shifts of the encoded itinerary. Each test of the inequality requires that we loop over the entire itinerary, so the complexity of checking the admissibility of the itinerary is $O((n-1)(n)) = O(n^2)$

Since we perform a $O(n^2)$ admissibility test on either $\sum_{j=0}^{(n-4)/2} \binom{n-2}{2j+1}$ or $\sum_{j=0}^{(n-3)/2} \binom{n-2}{2j+1}$ candidate itineraries, the overall time complexity of generating all admissible itineraries of length n is at most

$$O(n^2 \sum_{j=0}^{(n-3)/2} \binom{n-2}{2j+1}) \leq O(n^2 2^n).$$

It is worth noting that we perform a reducibility check on the encoded itineraries as we iterate for admissiblity. This reducibility check removes almost all duplicates from the data set without increasing the time complexity as the check only increases the admissiblity loop's runtime by a constant factor which, in practice, is very close to 1.

Encoding the itineraries does not change the space complexity of generating all admissible itineraries of length n because we still need to store at least $\sum_{j=0}^{(n-3)/2} \binom{n-2}{2j+1}$ candidate itineraries. If the itineraries were stored

[4] `https://docs.python.org/3/library/itertools.html#itertools.combinations`

unencoded, there would be in the worst case $\sum_{j=0}^{(n-4)/2} \binom{n-2}{2j+1}$ itineraries of space $O(n)$ for a total space complexity of space $O(n \sum_{j=0}^{(n-4)/2} \binom{n-2}{2j+1})$.

Encoded itineraries still take up $O(n)$ space in the worst case (consider the case where nearly all entries in the corresponding itinerary are 1's). So, the space complexity of generating all admissible itineraries of length n is $O(n \sum_{j=0}^{(n-4)/2} \binom{n-2}{2j+1}) \leq O(n2^n)$. However, encoding the itineraries significantly decreases the amount of space used by a large constant factor because only approximately half of the entries in an itinerary are expected to be 1's.

These inefficient time and space complexities are unavoidable because the number of admissible itineraries of length n appears to be itself exponential. In other words, the runtime of iterating over a list of admissible itineraries of length n (instead of up to n) will be exponential with respect to n.

8. Entropy of tent map

The entropy of the tent map with growth rate β is well-known to be $\log \beta$ in greater generality, following a theorem of Misieurwicz-Szlenk [MS77]. However, inspired by [But14], we adapt more elementary mathematical tools and proved this by constructing r-nacci numbers.

Define $I = [0, 1]$, let (I, d) be a compact metric space with metric

$$d_n(x, y) = \max_{0 \leq k < n} d(f^k(x), f^k(y)).$$

Note that the diameter of a set in I is the supremum of distances measured by d_n between the points in the set. The entropy of f can be defined by the minimal cardinality of a covering of I. Fixing $\epsilon > 0$, let $\text{cov}(n, \epsilon, f)$ denote the minimal cardinality of a covering of I by sets with d_n-diameter less than ϵ, the entropy of f can be written as a function of $\text{cov}(n, \epsilon, f)$.

Definition 8.1 (Entropy)**.** The *entropy* of a map f, denoted $h_\epsilon(f)$, is given by

$$h_\epsilon(f) = \limsup_{n \to \infty} \frac{1}{n} \log(\text{cov}(n, \epsilon, f)).$$

We will calculate the entropy of the tent map by finding upper and lower bounds for $h_\epsilon(f_\beta)$ and show they are equal. The following definitions will aid us in this approach.

Fix $\epsilon > 0$ and let $n \in \mathbb{N}$. We define a set $A \subset X$ to be an (n, ϵ)-*spanning set* provided that for all $x \in X$, there exists $y \in A$ such that $d_n(x, y) < \epsilon$. Additionally, we define a set $A \subset X$ to be an (n, ϵ)-*separated set* provided that for all $x, y \in A$ with $x \neq y$, $d_n(x, y) \geq \epsilon$. Denote the minimum cardinality of an (n, ϵ)-spanning set as $\text{span}(n, \epsilon, f)$ and the maximum cardinality of an (n, ϵ)-separated set as $\text{sep}(n, \epsilon, f)$.

Since

$$\lim_{n \to \infty} \frac{1}{n} \log(\text{sep}(n, \epsilon, f)) = h_\epsilon(f) = \lim_{n \to \infty} \frac{1}{n} \log(\text{span}(n, \epsilon, f)),$$

we can find the upper and lower bounds of $h_\epsilon(f)$ by computing the cardinality of two constructed spanning and separated sets. In this paper, we will first construct the spanning and separating sets, and then compute their cardinality and determine our bounds.

The proof for the upper bound being $\log \beta$ is a mild modification of Karen Butt's paper, and the full calculation is available to the reader in appendix D.1. In the following section, we find the lower bound by constructing separated sets and r-nacci numbers.

8.1. **Separated set.** Let $m = n-1+k$, and let I_m denote the set of dyadic rationals with denominator β^m, defined as

$$I_m := \left\{ \frac{i}{\beta^m} : 0 \leq i \leq \lfloor \beta^m \rfloor \right\}.$$

For $i \in \mathbb{N}$, let $c_{i,\epsilon}$ be the set where the image of f_β^i lies within an ϵ-neighborhood of $\frac{1}{\beta}$. Then,

$$c_{j,\epsilon} = \left\{ x \in X : f_\beta^j(x) \in [\frac{1}{\beta} - \frac{\epsilon}{2}, \frac{1}{\beta} + \frac{\epsilon}{2}] \right\}.$$

Let S_m be the set such that none of its elements lie within the ϵ-neighborhood of $\frac{1}{\beta}$ within n times of iteration,

$$S_{m,\epsilon} = I_m \setminus \sum_{j=0}^{n-1} (c_{j,\epsilon} \cap I_m).$$

Now, we make the following claim.

Proposition 8.2. *For all $\epsilon > 0$, there exists $k \in \mathbb{N}$ such that $S_{n-1+k,\epsilon}$ is a (n, ϵ)-separated set for f_β.*

Proof. See Appendix D.3. □

8.2. **Lower bound.** We calculate the cardinality of $S_{m,\epsilon}$, where $m = n - 1 + k$, by subtracting the cardinality of $c_{j,\epsilon} \cap I_m$ for all $0 \leq j \leq n-1$ from the cardinality of I_m. We see,

$$|S_{m,\epsilon}| = |I_m| - \sum_{j=0}^{n-1} |c_{j,\epsilon} \cap I_m| = \lfloor \beta^n \rfloor - \sum_{j=0}^{n-1} |c_{j,\epsilon} \cap I_m|.$$

Let t_j be the number of values of x such that $f_\beta^j(x) = 1$.

Since β is not an integer, I_m is not distributed uniformly over $[0, 1]$, we introduce

$$\max_{[a,b] \subseteq [0,1] : b-a = \frac{\epsilon}{\beta^j}} |I_m \cap [a, b]|,$$

the cardinality of the intersection of I_m and the interval $[a, b]$ of length $\frac{\epsilon}{\beta^j}$ in $[0, 1]$ that contains the maximum number of elements in I_m. Then, we

have an upper bound of the number of elements in I_m such that $f_\beta^j(x) = 1$,

$$|c_{j,\epsilon} \cap I_m| \leq t_j \cdot \max_{[a,b]\subseteq[0,1]:b-a=\frac{\epsilon}{\beta^j}} |I_m \cap [a,b]|.$$

Since elements in I_m are distributed evenly on $[0, \frac{\lfloor \beta^m \rfloor}{\beta^m}]$, we have

$$\max_{[a,b]\subseteq[0,1]:b-a=\frac{\epsilon}{\beta^j}} |I_m \cap [a,b]| \leq \frac{\epsilon/\beta^j}{1/\beta^m} = \epsilon\beta^{m-j}.$$

Therefore,

$$|S_{m,\epsilon}| \geq \lfloor \beta^n \rfloor - \sum_{i=0}^{m-1} t_j \cdot \max_{[a,b]\subseteq[0,1]:b-a=\frac{\epsilon}{\beta^j}} |I_m \cap [a,b]| = \beta^n - 1 - \sum_{i=0}^{m-1} (t_i \cdot \epsilon \cdot \beta^{m-j}).$$

We will soon prove that t_i, where t_i is the number values of x such that $f_\beta^i(x) = 1$, is bounded above by a generalized Fibonacci number. First, however, we must prove the following lemma.

Lemma 8.3. *Let j be any integer such that $j > r$. If $f_\beta^i(x) < \frac{1}{\beta}$ for all i such that $j \leq i < j + r$, $f_\beta^{-1}(f_\beta^j(x)) = \frac{f_\beta^j(x)}{\beta}$.*

Proof. See appendix D.4 □

We are now ready to find the upper bound of t_i.

Definition 8.4 (r-nacci number)**.** An r-nacci sequence F_r is an integer sequence that starts with $r-1$ many 0's, after which each term is the sum of the previous r terms:

$$F_{r,n} = \begin{cases} 0 & 0 \leq n \leq r-1 \\ 1 & r \leq n \leq 2r-1 \\ \sum_{i=n-1-r}^{n-1} F_{r,i} & \text{otherwise} \end{cases}$$

For example, $F_{3,n} = (0, 0, 1, 1, 2, 4, 7, 13, 24, \dots)$ is the 3-nacci sequence.

Lemma 8.5. *Fix β and $r = \min\left\{r \in \mathbb{Z} \mid \frac{1}{\beta^r} \leq 2 - \beta\right\}$. Then, $t_i \leq F_{r,i+r}$.*

Proof. First, we will prove by induction that for any $i \geq r$, we have $t_i \leq \sum_{j=i-r}^{i-1} t_j$. Consider $i = 0, 1$ as our base cases. Since $x = 1$ is the only solution to $f_\beta^0(x)$, and $x = \frac{1}{\beta}$ is the only solution to $f_\beta^1(x)$, $t_0 = t_1 = 1$. Let f_β^{-j} denote the preimage of f_β^j. For any $j \in (0, r] \cap \mathbb{N}$, since $f_\beta^{-j}(1) \geq \frac{1}{\beta^r} \geq 2 - \beta$, we have $0 < \frac{f_\beta^{-j}(1)}{\beta} < \frac{1}{\beta}$ and $\frac{1}{\beta} \leq \frac{2 - f_\beta^{-j}(1)}{\beta} \leq 1$. Therefore, there are always two elements in the preimage, $f_\beta^{-j}(x)$: $\frac{f_\beta^{-j}(1)}{\beta}$ and $\frac{2-f_\beta^{-j}(1)}{\beta}$. Thus, $t_j = 2^{j-1}$ for all $j \in (0, r] \cap \mathbb{N}$, and $t_r = 2^{r-1} = \sum_{j=0}^{r-1} t_j$.

By the induction hypothesis that for some $i \geq r$, $t_i \leq \sum_{j=i-r}^{i-1} t_j$, we see

$$t_{i+1} \leq 2t_i - t_{i-r} \leq t_i + \sum_{j=i-r}^{i-1} t_j - t_{i-r} = \sum_{j=i+1-r}^{i} t_j$$

which completes the inductive proof.

For a fixed β, we will then compare the ith term of (t_i) with the $(i+r)$th r-nacci number. Since

(1) $t_0 = 1 \leq F_{r,r} = 1$,
(2) For all $i \in (1, r-1] \cap \mathbb{N}$, $t_i = 2^{i-1} < F_{r,i+r} = 2^{i+r-1}$,
(3) $F_{r,i} = \sum_{i=n-1-r}^{n-1} F_{r,i}$ for all $i \geq r$,

we can conclude that $t_i \leq F_{r,i+r}$ for all $i \geq 0$. □

Since t_i is bounded above by $F_{r,i+r}$, $|S_{n-1+k,\epsilon}|$ is bounded below:

$$\begin{aligned}
|S_{n-1+k,\epsilon}| &\geq \beta^{n-1+k} - 1 - \sum_{i=0}^{n-1+k-1} t_i \cdot \epsilon \cdot \beta^{n-1+k-i} \\
&\geq \beta^{n-1+k} - 1 - \epsilon \left(\sum_{i=0}^{n-1+k-1} F_{r,i+r} \cdot \beta^{n-1+k-i} \right) \\
&\geq \beta^{n-1+k} - 1 - \frac{\beta^{n+k-1+r}}{\beta^k} \left(\sum_{i=0}^{n-1+k-1} F_{r,i+r} \cdot \beta^{-(i+r)} \right),
\end{aligned}$$

since $\frac{1}{\beta^{k+1}} \leq \epsilon \leq \frac{1}{\beta^k}$ by construction.
Therefore,

$$\begin{aligned}
h_\epsilon(f_\beta) &= \lim_{n\to\infty} \frac{1}{n} \log(\mathrm{sep}(n, \epsilon, f_\beta)) \geq \lim_{n\to\infty} \frac{1}{n} \log(|S_{n-1+k}|) \\
&\geq \lim_{n\to\infty} \frac{1}{n} \log \left(\beta^{n-1+k} - 1 - \beta^{n-1+r} \left(\sum_{i=0}^{\infty} F_{r,i+r} \cdot \beta^{-(i+r)} \right) \right).
\end{aligned}$$

Let $S = \sum_{i=0}^{\infty} F_{r,i+r} \cdot \beta^{-(i+r)}$. Then,

$$\begin{aligned}
&S - \beta^{-1}S - \beta^{-2}S - \cdots - \beta^{-r}S \\
=&\sum_{i=0}^{\infty} F_{r,i+r} \cdot \beta^{-(i+r)} - \sum_{i=1}^{\infty} F_{r,i+r-1} \cdot \beta^{-(i+r)} - \cdots - \sum_{i=r}^{\infty} F_{r,i} \cdot \beta^{-(i+r)} \\
=&(F_{r,r} + F_{r,r+1}\beta^{-1} + \cdots + F_{r,2r-1}\beta^{-(r-1)} + \sum_{i=r}^{\infty} F_{r,i+r} \cdot \beta^{-(i+r)}) \\
&- (F_{r,r}\beta^{-1} + F_{r,r+1}\beta^{-2} + \cdots + F_{r,2r-2}\beta^{-(r-1)} + \sum_{i=r}^{\infty} F_{r,i+r-1} \cdot \beta^{-(i+r)}) \\
&- \cdots - \sum_{i=r}^{\infty} F_{r,i} \cdot \beta^{-(i+r)}.
\end{aligned}$$

Hence, we have

$$\begin{aligned}
&S - \beta^{-1}S - \beta^{-2}S - \cdots - \beta^{-r}S \\
=&(F_{r,r} + F_{r,r+1}\beta^{-1} + \cdots + F_{r,2r-1}\beta^{-(r-1)}) \\
&-(F_{r,r}\beta^{-1} + F_{r,r+1}\beta^{-2} + \cdots + F_{r,2r-2}\beta^{-(r-1)}) - \cdots - (F_{r,r}\beta^{-(r-1)}) \\
&+(\sum_{i=r}^{\infty} F_{r,i+r} \cdot \beta^{-(i+r)} - \sum_{i=r}^{\infty} F_{r,i+r-1} \cdot \beta^{-(i+r)} - \cdots - \sum_{i=r}^{\infty} F_{r,i} \cdot \beta^{-(i+r)})
\end{aligned}$$

Since $F_{r,i+r} = F_{r,i+r-1} + F_{r,i+r-2} + \cdots + F_{r,i}$ by definition,

$$\sum_{i=r}^{\infty} F_{r,i+r} \cdot \beta^{-(i+r)} - \sum_{i=r}^{\infty} F_{r,i+r-1} \cdot \beta^{-(i+r)} - \cdots - \sum_{i=r}^{\infty} F_{r,i} \cdot \beta^{-(i+r)} = 0.$$

Therefore,

$$\begin{aligned}
&S - \beta^{-1}S - \beta^{-2}S - \cdots - \beta^{-r}S \\
=&(2^0 + 2^1\beta^{-1} + \cdots + 2^{(r-1)}\beta^{-(r-1)}) - (2^0\beta^{-1} + \cdots + 2^{(r-2)}\beta^{-(r-1)}) \\
&- \cdots - 2^0\beta^{-(r-1)} + 0 = 1 + \beta^{-1} + \beta^{-2} + \cdots + \beta^{-(r-1)}.
\end{aligned}$$

This implies,

$$S = \frac{\frac{1-\beta^{-r}}{1-\beta^{-1}}}{1 - (\beta^{-1} + \beta^{-2} + \cdots + \beta^{-r})}.$$

So, we see

$$\begin{aligned}
h_\epsilon(f_\beta) &\geq \beta^{n-1+k} - 1 - \frac{\beta^{n+k-1+r}}{\beta^k} \left(\sum_{i=0}^{n-1+k-1} F_{r,i+r} \cdot \beta^{-(i+r)} \right) \\
&\geq \beta^{n-1+k} - 1 - \frac{\beta^{n+k-1+r}}{\beta^k} \left(\frac{\frac{1-\beta^{-r}}{1-\beta^{-1}}}{1 - (\beta^{-1} + \beta^{-2} + \cdots + \beta^{-r})} \right).
\end{aligned}$$

Since

$$\lim_{n\to\infty} \frac{1+\beta^{n-1+r}\cdot \frac{\frac{1-\beta^{-r}}{1-\beta^{-1}}}{1-(\beta^{-1}+\beta^{-2}+\ldots\beta^{-r})}}{\beta^{n-1+k}} = c,$$

for some constant c, we will have

$$\begin{aligned} h_\epsilon(f_\beta) &= \lim_{n\to\infty}\frac{1}{n}\log(\mathrm{sep}(n,\epsilon,f_\beta)) \\ &\geq \lim_{n\to\infty}\frac{1}{n}\log\left(\beta^{n-1+k}-1-\beta^{n-1+r}\cdot\frac{\frac{1-\beta^{-r}}{1-\beta^{-1}}}{1-(\beta^{-1}+\beta^{-2}+\ldots\beta^{-r})}\right) \\ &= \lim_{n\to\infty}\frac{\log c+n-1+k}{n}\log(\beta)=\log\beta. \end{aligned}$$

Since the entropy of tent map has a upper bound of $\log\beta$ and a lower bound of $\log\beta$, by the squeeze theorem for limits, $h_{\epsilon\to 0^+}(f_\beta)$ exists and is equal to $\log\beta$.

Appendix A. Methodology

To generate all possible candidate encodings, we use Python's itertools library. Itertools provides a set of fast and memory-efficient tools for iterating over various combinations and permutations. In particular, we used itertools' combinations function when looping over possible itineraries. This function, when passed a list and a length r, returns all subsequences of length r from the list. While the combinations function is efficient from a theory of computation perspective, it is one of our biggest runtime pain points due to the unavoidably large number of possible combinations it returns.[5]

Appendix B. Distribution of Itineraries

Our data set contains 269,017,181 unique itineraries. They are distributed across orbit lengths 3 - 33 as follows:

n	# Itineraries
3	1
4	1
5	3
6	4
7	9
8	14
9	28
10	48
11	93
12	165
13	315
14	576
15	1,091
16	2,032
17	3,855
18	7,252
19	13,797
20	26,163
21	49,929
22	95,232
23	182,361
24	349,350
25	671,088
26	1,290,240
27	2,485,504
28	4,792,905
29	9,256,395
30	17,894,588
31	34,636,833
32	67,106,816
33	130,150,493

[5] `https://docs.python.org/3/library/itertools.html`

Appendix C. Additional Visualizations from Subsection 6.4.3

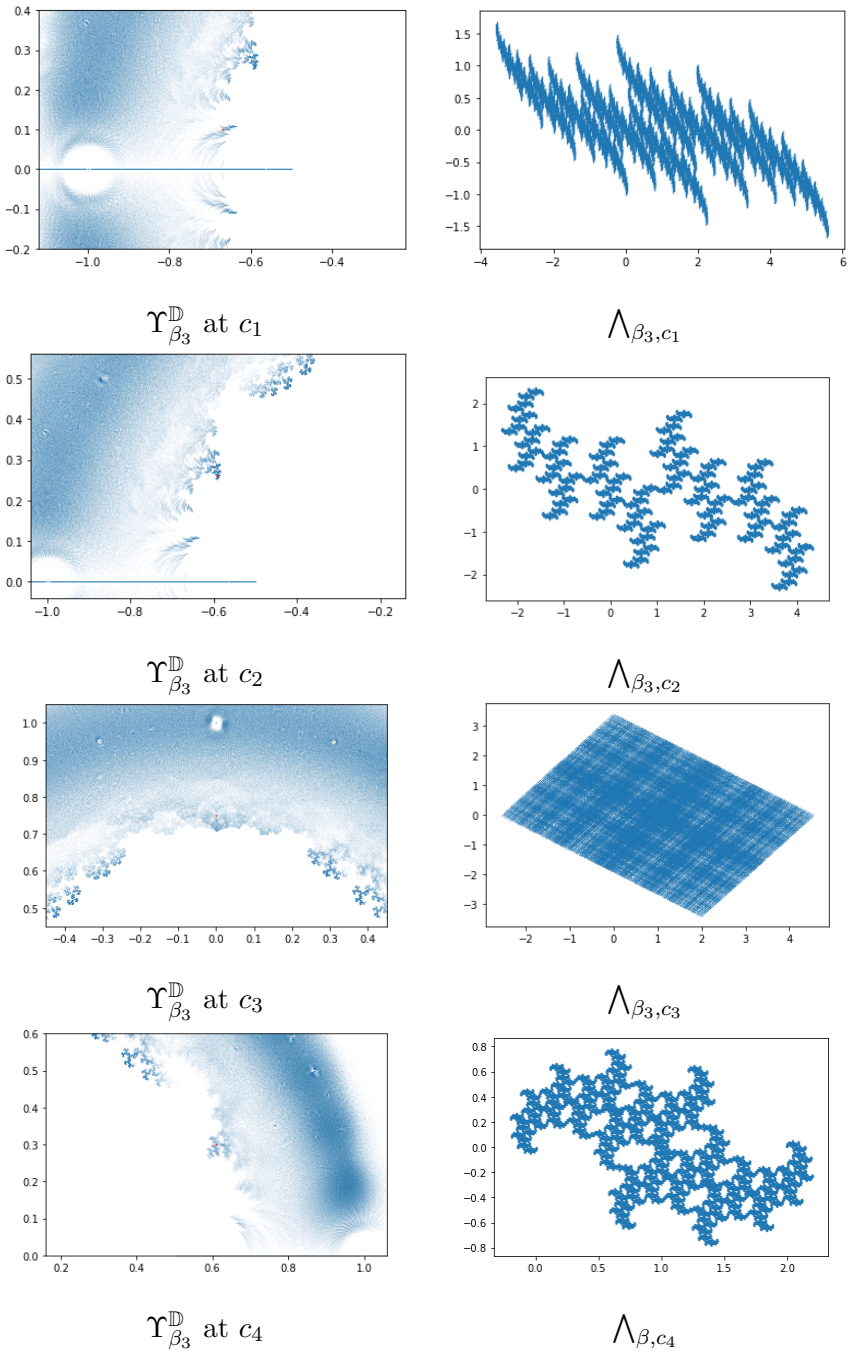

Figure 10. Varied values of c for fixed β.

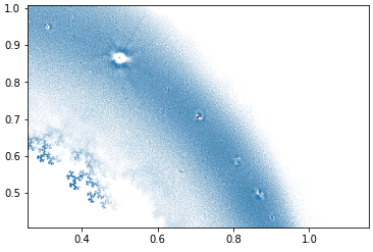

$\Upsilon^{\mathbb{D}}_{\beta_3}$ at c_5

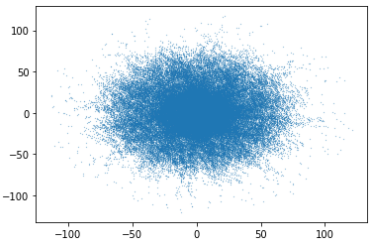

$\bigwedge_{\beta_3,c_5}$

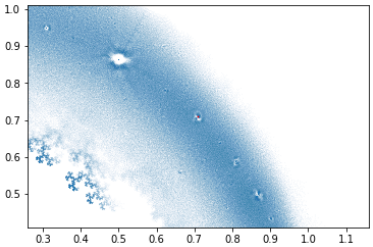

$\Upsilon^{\mathbb{D}}_{\beta_3}$ at c_6

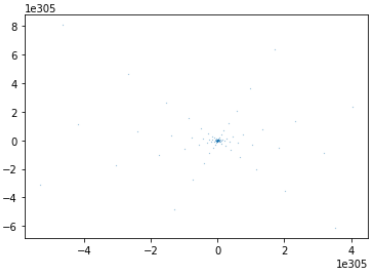

$\bigwedge_{\beta_3,c_6}$

FIGURE 11. Approximations for c near the roots of unity.

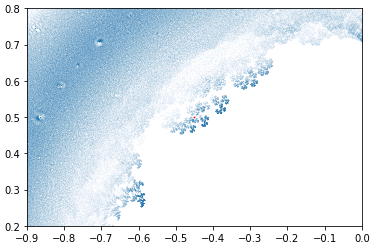

$\bigwedge_{\beta_3,c_7}$

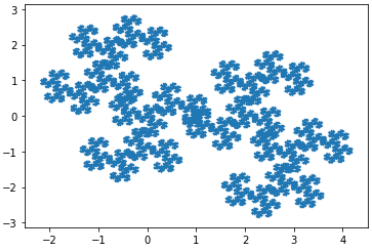

$\bigwedge_{\beta_3,c_7}$

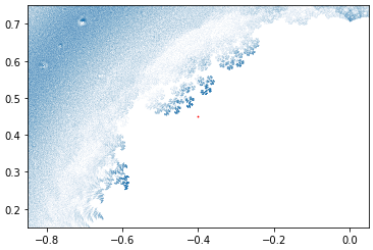

$\bigwedge_{\beta_3,c_8}$

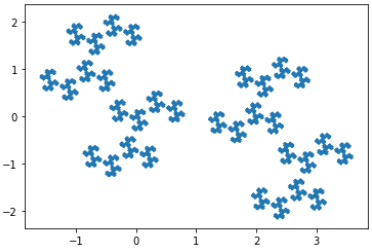

$\bigwedge_{\beta_3,c_8}$

FIGURE 12. Approximations for c inside and outside the Thurston Set.

Appendix D. Additional proof for Entropy of Tent Map

D.1. **Upper bound on entropy.**

D.1.1. *Spanning set.* Let I_m denote the set of dyadic rationals with denominator β^m, defined as

$$I_m := \left\{ \frac{i}{\beta^m} : 0 \leq i < \lfloor \beta^m \rfloor \right\}.$$

To prove the set of fractions I_{n+k} is an (n, ϵ)-spanning set for the tent map, we first prove the following lemma.

Lemma D.1. *Let f_β be the tent map of slope β. Then,*

$$d(f_\beta(x), f_\beta(y)) \leq \beta d(x, y).$$

Proof. For all $x, y \in I$, we see

$$d(f_\beta(x), f_\beta(y)) = |1 - \beta x| - |1 - \beta y|.$$

Notice,

$$|1 - \beta x| \geq \beta |x - y| + |1 - \beta y|.$$

Therefore,

$$|1 - \beta x| - |1 - \beta y| \leq \beta d(x, y).$$

□

Now, we are prepared to show I_{n+k} is an (n, ϵ)-spanning set.

Proposition D.2. *For all $\epsilon > 0$, there exists a $k \in \mathbb{N}$ such that I_{n+k} is an (n, ϵ)-spanning set for f_β.*

Proof. Fix $\epsilon > 0$. Choose $k \geq 2$ such that $\frac{1}{\beta^{k+1}} \leq \epsilon < \frac{1}{\beta^k}$. Note that for any $x \in I$, there exists $i \in \{0, \ldots, \beta^{n+k} - 1\}$ such that

$$x \in [\frac{i}{\beta^{n+k}}, \frac{i+1}{\beta^{n+k}}).$$

Then, choose $y \in I_{n+k}$ to be either of the endpoints of this dyadic interval. Thus,

$$d(x, y) \leq \frac{1}{\beta^{n+k}}.$$

By Lemma D.1, this implies

$$d(f_\beta(x), f_\beta(y)) \leq \beta d(x, y) \leq \frac{\beta}{\beta^{n+k}}.$$

Applying Lemma D.1 j consecutive times, for any $0 \leq j < n$, yields

$$d(f_\beta^j(x), f_\beta^j(y)) = \beta^j d(x, y) < \frac{\beta^j}{\beta^{n-k}} < \frac{\beta^n - 1}{\beta^{n-k}} < \frac{1}{\beta^{k+1}} \leq \epsilon.$$

So, for any $x \in I$, we have,

$$\max_{0 \leq j < n} (d(f_\beta^j(x), f_\beta^j(y))) = d_n(x, y) < \epsilon,$$

for some $y \in I_{n+k}$. Therefore, I_{n+k} is an (n, ϵ)-spanning set for f_β. □

D.1.2. *Upper bound.* As I_{n+k} is a (n, ϵ)-spanning set (Proposition D.2) and the numerators of the fractions range from 0 to $\beta^{n+k} - 1$, we see I_{n+k} has cardinality β^{n+k}. Therefore, $\text{span}(n, \epsilon, f_\beta) \leq \beta^{n+k}$. Thus,

$$\begin{aligned} h_\epsilon(f_\beta) &= \lim_{n\to\infty} \frac{1}{n} \log(\text{span}(n, \epsilon, f_\beta)) \\ &\leq \lim_{n\to\infty} \frac{(n+k)\log\beta}{n} \\ &= \log\beta. \end{aligned}$$

D.2. **Propositions and Lemmas.**

Proposition D.3. *For all $\epsilon > 0$, there exists $k \in \mathbb{N}$ such that $S_{n-1+k,\epsilon}$ is a (n, ϵ)-separated set for f_β.*

Proof. Fix $\epsilon > 0$. Choose $k \geq 2$ such that $\frac{1}{\beta^{k+1}} \leq \epsilon < \frac{1}{\beta^k}$. Let x, y be two distinct points in $S_{n-1+k,\epsilon}$. We want to show that $d_n(x, y) \geq \epsilon$ for all such x, y. To do this, we must prove that there exists $0 \leq j \leq n-1$ such that $d(f_\beta^j(x), f_\beta^j(y)) \geq \epsilon$. We break this into two cases.

First, suppose there exists $j \in \mathbb{N}$, $0 \leq j \leq n$, such that $f_\beta^j(x) < \frac{1}{\beta} < f_\beta^j(y)$. Without loss of generality, we assume that $f_\beta^j(x) < f_\beta^j(y)$. Then, $d_j(x, y) > \epsilon$ by design so our claim holds for this case.

Next, instead suppose that for all $j \in \mathbb{N}$, $0 \leq j \leq n$,

$$(f_\beta^j(x) - \frac{1}{\beta}) \cdot (f_\beta^j(y) - \frac{1}{\beta}) > 0.$$

Under these circumstances, it is always true that

$$d(f_\beta(x), f_\beta(y)) = \beta d(x, y).$$

After applying this equality $n-1$ times, we see

$$d(f_\beta^{n-1}(x), f_\beta^{n-1}(y)) = \beta^{n-1} d(x, y).$$

Note that for all distinct $x, y \in S_{n-1+k}$, we have $d(x, y) \geq \frac{1}{\beta^{n-1+k}}$, which implies

$$\beta^{n-1} d(x, y) \geq \frac{\beta^{n-1}}{\beta^{n-1+k}} = \frac{1}{\beta^k} > \epsilon.$$

Therefore, S_{n-1+k} is an (n, ϵ)-separated set for f_β. □

Lemma D.4. *Let j be any integer such that $j > r$. If $f_\beta^i(x) < \frac{1}{\beta}$ for all i such that $j \leq i < j + r$, $f_\beta^{-1}(f_\beta^j(x)) = \frac{f_\beta^j(x)}{\beta}$.*

Intuitively, Lemma D.4 means that, if the preimage of $f_\beta^i(x)$ is $\frac{f_\beta^i(x)}{\beta}$ for r consecutive iterations, then the preimage of $f_\beta^j(x)$, where nonnegative j is

less than the least value i in the chain of r iterates, must be $\left\{\frac{f_\beta^j(x)}{\beta}\right\}$. We will use this understanding in our proof.

Proof. As the preimage of $f_\beta^j(x)$ is a subset of $\left\{\frac{f_\beta^j(x)}{\beta}, \frac{2-f_\beta^j(x)}{\beta}\right\}$, it is equivalent to prove that the preimage of $f_\beta^j(x)$ does not contain $\frac{2-f_\beta^j(x)}{\beta}$. We can do this by showing that $\frac{2-f_\beta^j(x)}{\beta} > 1$. If $f_\beta^i(x) < \frac{1}{\beta}$ for all i such that $j \le i < j+r$, then the preimage of $f_\beta^{i+1}(x)$ is $\frac{f_\beta^{i+1}(x)}{\beta}$ for all such i. Therefore,

$$f_\beta^j(x) = \frac{f_\beta^{j+r}(x)}{\beta^{j+r-j}} < \frac{1}{\beta^r} < 2-\beta.$$

Thus,

$$\frac{2-f^j(x)}{\beta} \ge \frac{1-\frac{1}{\beta^r}}{\beta} > \frac{2-2+\beta}{\beta} = 1,$$

which completes the proof. □

If $f_\beta^{-1}(f_\beta^i(x)) = \left\{\frac{f_\beta^i(x)}{\beta}, \frac{2-f_\beta^i(x)}{\beta}\right\}$ for all $i < j$, then we have $t_i = 2t_{i-1}$. Intuitively, this means that if the preimage of $f_\beta^i(x)$ always has two elements, $\frac{f_\beta^i(x)}{\beta}$ and $\frac{2-f_\beta^i(x)}{\beta}$, then the number of values of x such that $f_\beta^i(x) = 1$ is twice of the number of values of x such that $f_\beta^{i-1}(x) = 1$. However, Lemma D.4 proves that this two-element preimage is not always the case. Also, if $f_\beta^i(x) < \frac{1}{\beta}$ for all i such that $j \le i < j+r$, then $f_\beta^{j-1}(x) = \frac{f_\beta^j(x)}{\beta}$. Therefore, for all i, we have $t_i \le 2 \cdot t_{i-1} - t_{i-r-1}$.

References

[BBBP98] Frank Beaucoup, Peter Borwein, David W. Boyd, and Christopher Pinner. Multiple roots of $[-1, 1]$ power series. *J. London Math. Soc. (2)*, 57(1):135–147, 1998.

[BDLW19] Harrison Bray, Diana Davis, Kathryn Lindsey, and Chenxi Wu. The Shape of Thurston's Master Teapot. 2019.

[But14] Karen Butt. An introduction to topological entropy. 2014.

[CKW17] Danny Calegari, Sarah Koch, and Alden Walker. Roots, Schottky semigroups, and a proof of Bandt's conjecture. *Ergodic Theory Dynam. Systems*, 37(8):2487–2555, 2017.

[Lei90a] Tan Lei. Similarity between the mandelbrot set and julia sets. *Communications in Mathematical Physics*, 134:587–617, 1990.

[Lei90b] Tan Lei. Similarity between the mandelbrot set and julia sets. *Comm. Math. Phys.*, 134(3):587–617, 1990.

[LW19] Kathryn Lindsey and Chenxi Wu. A characterization of Thurston's Master Teapot. 2019.

[MS77] M. Misiurewicz and W. Szlenk. Entropy of piecewise monotone mappings. In *Systèmes dynamiques II - Varsovie*, number 50 in Astérisque. Société mathématique de France, 1977.

[MT88] John Milnor and William Thurston. On iterated maps of the interval. In *Dynamical systems (College Park, MD, 1986–87)*, volume 1342 of *Lecture Notes in Math.*, pages 465–563. Springer, Berlin, 1988.

[Par60] W. Parry. On the β-expansions of real numbers. *Acta Math. Acad. Sci. Hungar.*, 11:401–416, 1960.

[Par66] William Parry. Symbolic dynamics and transformations of the unit interval. *Trans. Amer. Math. Soc.*, 122:368–378, 1966.

[Tho16] Daniel Thompson. Generalized beta-transformations and the entropy of unimodal maps. *Commentarii Mathematici Helvetici*, 92:777–800, 02 2016.

[Thu14] William P. Thurston. Entropy in dimension one. In *Frontiers in complex dynamics*, volume 51 of *Princeton Math. Ser.*, pages 339–384. Princeton Univ. Press, Princeton, NJ, 2014.

[Tio20] Giulio Tiozzo. Galois conjugates of entropies of real unimodal maps. *International Mathematics Research Notices*, 2020:607–640, 2020.

Acknowledgements. *The authors wish to thank the Laboratory of Geometry at Michigan for facilitating this research. Also, Dr. Harrison Bray and Samuel Hansen for their invaluable assistance and support.*

Robert Buckley, robuckle@umich.edu, The University of Michigan
Yiwang Chen, yiwchen@umich.edu, The University of Michigan
Grace O'Brien, graceob@umich.edu, The University of Michigan
Zoe Zhou, zoezhou@umich.edu, The University of Michigan